

A scalable scanning transfer cavity laser stabilization scheme based on the Red Pitaya STEMLab platform

E. Pultinevicius, M. Rockenhäuser, F. Kogel, P. Groß, T. Garg, O. E. Prochnow, and T. Langen

5. Physikalisches Institut and Center for Integrated Quantum Science (IQST),
Pfaffenwaldring 57, Universität Stuttgart, 70569 Stuttgart, Germany

(*t.langen@physik.uni-stuttgart.de)

(Dated: July 21, 2023)

Many experiments in atomic and molecular physics require simultaneous frequency stabilization of multiple lasers. We present a stabilization scheme based on a scanning transfer cavity lock that is simple, stable and easily scalable to many lasers at minimal cost. The scheme is based on the *Red Pitaya STEMLab* platform, with custom software developed and implemented to achieve up to 100Hz bandwidth. As an example demonstration, we realize simultaneous stabilization of up to four lasers and a reduction of long-term drifts to well below 1 MHz per hour. This meets typical requirements, e.g. for experiments on laser cooling of molecules.

I. INTRODUCTION

Laser frequency stabilization is an important component of many scientific investigations and technological applications of atoms and molecules. A large variety of techniques exist to stabilize a laser to an atomic resonance [1–4] or optical resonator [5–8], ranging from simple spectroscopic schemes to the millihertz-level techniques used to realize the most precise optical clocks [9, 10] and gravitational interferometers [11].

However, advanced methods for laser stabilization can be complex and expensive, while in many experiments only moderate precision and bandwidth are required. A recent example are experiments aiming to laser cool molecules [12–14]. In comparison to atoms, molecules feature a much more complex level structure, where decay into undesired states needs to be compensated through — sometimes up to almost a dozen [15] — repumping lasers. At the same time, only moderate compensation against drifts on the order of the transition linewidths are required, typically in the range of a few MHz. For such experiments, stabilization schemes that are simple, robust and scalable to many lasers are thus highly desirable.

Here we present a scanning transfer cavity lock which is ideally suited to meet these requirements. Our approach utilizes the readily available, high-resolution analog-to-digital converter and fast digital signal processing capabilities of the *Red Pitaya* (RP) *STEMLab* platform [16]. Combining this with a simple Fabry-Perot cavity enables long-term sub-MHz-level frequency stabilization using a simple setup, which we demonstrate for up to four lasers in parallel. Our scheme offers a cost-effective and scalable solution for stabilizing lasers that is applicable to a large variety of experiments.

II. LOCKING SCHEME

The basic setup for our laser frequency stabilization scheme is shown in Fig. 1. It is based on the well-established, generic concept of a scanning transfer cavity lock (STCL). Beams from several lasers are superimposed and their transmission through a scanning Fabry-Perot cavity is monitored [17]. One of the lasers is frequency stabilized and serves as a reference for the scheme. This initial frequency stabilization can be re-

alized by locking the reference laser to an atomic vapor spectroscopy or by using an inherently frequency-stable laser, such as a helium-neon laser. The positions of the cavity transmission peaks of this reference are then stabilized by changing the cavity length. This transfers the frequency stability of the reference laser to the cavity and stabilizes it against drifts. The positions of all other transmission peaks on this — now precisely controlled — frequency scale are subsequently used to generate feedback, by means of which the corresponding lasers are stabilized.

III. IMPLEMENTATION

Similar STCL schemes have been widely used in many experiments in atomic and molecular physics [18–23]. Here, we employ RP units for a simple, cost-effective and fully digital processing of the transmission data of the transfer cavity.

The RP is a multi-instrument, FPGA based platform with open-source capabilities. Fast analog-in and output channels make it very suitable for the processing of analog signals. In the context of laser stabilization, a powerful toolkit is provided for this platform by the *PyRPL python* package [24]. In terms of cavity stabilization, this package provides, e.g., an interface for analog-to-digital conversion, signal processing and generation. In principle, this makes the package suitable for realizing a STCL, but it also requires permanent data transfer between the RP platform and a personal computer (PC) for signal processing that is not carried out on the FPGA itself. If applied to setups with many lasers, this typically creates a large data transfer overhead that limits the realizable bandwidth of the stabilization. Our solution aims to minimize this data overhead, by performing all processing and monitoring tasks directly on the RP's internal CPU. It also minimizes the complexity of the optical setup by using only a single cavity for a potentially large number of lasers, and does not require any additional radio-frequency components.

To realize the locking, several RP units are operated in a stand-alone way, where only the basic control commands to run and control the STCL locking loop are externally provided by the user via a local area network (LAN) connection. This connection is realized using *Python* modules that are run on

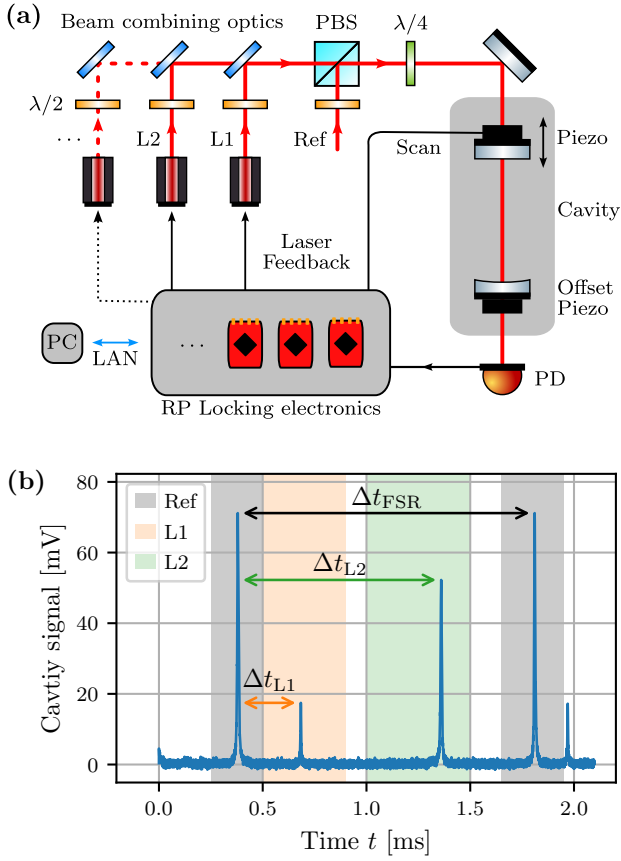


FIG. 1. **(a)** Scheme of the scanning transfer cavity lock. A stable reference laser (Ref) is used to stabilize the length of a scanning Fabry-Perot cavity by recording the laser's cavity transmission signal on a photodiode (PD). Other lasers (L1, L2, or several more indicated by dotted lines) are superimposed with this laser on the cavity through polarizing and dichroic optics, in order to be frequency stabilized. An additional quarter-wave plate minimizes optical feedback from the cavity reflection back into the lasers. **(b)** Transmission signal of the lasers when scanning the cavity length with the piezo actuator. The peak positions of the reference laser (peaks in gray-shaded regions, separated by one free spectral range of the cavity) provide feedback to stabilize the length of the cavity. This feedback is realized by adding a suitable bias voltage to the scanning cavity piezo to always keep these peaks in the same location. The transmission peaks of any other lasers are detected in their respective regions of interest (color-shaded regions) and their pre-defined, relative distances to the reference laser (indicated by arrows) are kept constant by providing feedback. All feedback signals are generated using synchronized RP units that are remote-controlled by the user through a PC. Before engaging the lock, any potential overlap between the transmission peaks of different lasers can be removed by shifting the wavelength-dependent resonance condition of the cavity by several free-spectral ranges through a second offset piezo actuator (see Appendix A).

both the RP units and the PC. In our scheme, we use a script to host servers on the RP via *Python's socket* package. We then employ an interface available on the RP for the use in *Jupyter* notebooks, which provides access to the FPGA functions. With that, the analog input and output channels can be controlled directly through the RP platform's CPU.

A schematic illustration of components operated on the RP units, on the controlling PC, as well as their mutual communication is shown in Fig. 2. The basic setup requires one RP (*RP Cavity*) for the scan and stabilization of the transfer cavity to the reference laser. Every pair of additional lasers on the same cavity then requires one additional device (*RP Laser*), since each RP features two fast analog outputs and can thus provide feedback for two lasers.

The cavity is scanned by bursts of triangular signals, generated using the signal generation capabilities of RP Cavity's FPGA. The frequency of the waveform (238 Hz) is chosen such that the period is a multiple of the minimum acquisition duration of the FPGA's inputs (In1 and In2). This way the acquisition time can be matched to the duration of the upwards slope. During the signal processing, the cavity piezo can settle back to its original length throughout the downwards slope. The signal acquisition and processing is triggered on all devices using a square wave, synchronized to the cavity scan and generated on the second output of RP Cavity.

The detected cavity transmission is evaluated on the CPU of RP Cavity. This involves the determination of different resonance positions that need to be distinguished from one another. For that purpose, regions of interest are specified for the respective lasers in the cavity (see Fig. 1b). The peaks are then detected by searching for the maximum positions in the respective ranges. Using the data points next to those positions, a Savitzky-Golay derivative filter [25] is applied. The resulting zero-crossing is determined using linear regression to find the resonance position [20]. This method efficiently smoothens the data around the resonance and increases the time resolution of the peak detection algorithm. The ranges of interest as well as the necessary parameters for the peak-detection algorithm are remotely provided from a PC and are saved on the device.

From the evaluated peak positions for the reference laser and the lasers L_i the relative positions Δt_{L_i} (see Fig. 1b) are calculated to obtain the respective error signals

$$e_{L_i} = \frac{\Delta t_{L_i}}{\Delta t_{\text{FSR}}} - s_{L_i}. \quad (1)$$

The set values s_{L_i} are defined by the user. Variations of the scan ramp are cancelled out by the division over the FSR Δt_{FSR} of the cavity [20]. This includes effects that can arise due to the non-linearity and hysteresis of the cavity piezo. For cavity stabilization, the error e_{Ref} is simply defined as the distance of the resonance to a pre-defined set value.

In addition to the signal processing, the locking also requires a feedback loop, which is not directly available on the RP's FPGA. We thus implemented a dedicated digital proportional-integral-derivative controller (PID controller). As the aim of our locking scheme is to compensate against slow long-term drifts of laser frequencies, we use mainly the integral (I) and proportional (P) terms of this controller.

A drawback of our remote-controlled implementation of the lock is that the actual data on the RP can not be accessed while the lock is enabled without compromising locking bandwidth. For this reason an additional RP unit (*RP Monitor*) that is in-

their diode currents or through piezo actuators controlling the length of an external Littrow cavity. In cases where only small feedback is required and which may thus be limited by the 14bit resolution of the RP's output signal, this signal can be improved by combining higher output amplitudes with an attenuator. For the Ti:Sapphire laser the feedback was applied to a piezo actuator, which controls the length of an internal cavity of the laser.

For the transfer cavity, we typically used a simple home-built design in our tests [26]. It consists of a plane and a confocal mirror, which are separated by 165.4 mm using a stainless steel spacer, resulting in a free spectral range of 906 MHz. Given a particular wavelength range of interest, we used custom mirror coatings, resulting in a typical finesse on the order of 240. The mirrors of the cavity are mounted on piezo ring actuators, allowing for fine control of the resonator length. As indicated in Fig. 1a, the first piezo actuator was used for scanning and stabilization of the cavity length, while the second was used to realize a fixed length offset independently of the operation of the STCL.

This latter feature is useful to easily minimize the overlap of transmission peaks from different lasers and is thus crucial for the scalability of our scheme. As the transmission resonance condition for each laser depends on its wavelength, any incidental overlap between two peaks from different lasers can be removed simply by shifting the cavity length by several free-spectral ranges (see Appendix A). The same can also be achieved with a single piezo in combination with a bias voltage on the scan ramp.

It should be noted that the analog outputs of the RP are limited to a range of ± 1 V, which is not sufficient to drive a typical piezo actuator over its full range. For this reason, whenever necessary, we employed amplifiers to scale the voltages to sufficient amplitudes [27]. In the case of the transfer cavity, this solution not only allows for a variable gain and offset, which is useful for the initialization of the scanning range, but also reduces noise on the scanning ramp. Additional noise reduction is possible using a low-pass filter that is matched to the capacity of the piezo and the speed of the scan ramp.

Our scheme is not specific to a particular cavity design and can easily be realized also with any other cavity. In particular, cavities mounted in vacuum or constructed using low thermal expansion materials could further improve the performance of the lock presented in this work.

B. Basic locking

An example result for the stabilization of a home-built diode laser is illustrated in Fig. 3a. This laser was set close to a transition required for the laser cooling of barium monofluoride molecules that is located at 898 nm [28]. For the reference, a commercial diode laser was stabilized to the cesium D1 line at 895 nm via a vapor cell FM spectroscopy [2], which was implemented using *PyRPL* [24].

The error e of the laser frequency was evaluated from the cavity signals as in Eqn. 1, with the frequency scale obtained by multiplication with the free spectral range. In addition to

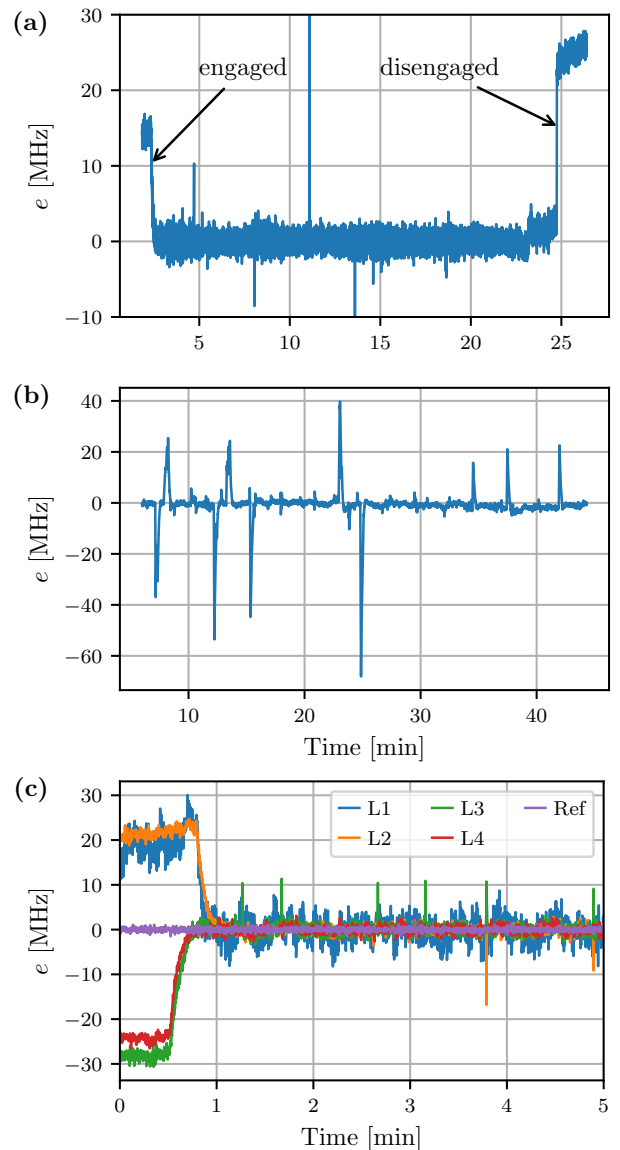


FIG. 3. **(a,b)** Example locking of a single laser. **(a)** Deviations from the setpoint measured on the transfer cavity over time. After the lock is engaged, the initial error rapidly decreases. During the lock, the error fluctuates around zero with a standard deviation of 0.91 MHz. After more than 20 min the lock is disengaged. Spikes are the result of small external perturbations which are rapidly compensated by the STCL. **(b)** Performance of the lock while the laser is purposely subjected to major external perturbations. Again, after each perturbation the lock rapidly returns the laser to the set frequency. This data was recorded using a wavemeter, which confirms the error evaluation performed on the RPs. **(c)** Operation of the STCL for four lasers. The fast noise visible at L1 is the result of a particularly noisy homemade diode laser, which, like L2-L4, could be successfully stabilized.

the internal monitoring of the STCL, the frequency scale and the operation of the lock were also independently observed and validated using a wavemeter throughout the tests.

In order to illustrate the difference between the locked and unlocked states, the lock was intentionally operated for a time

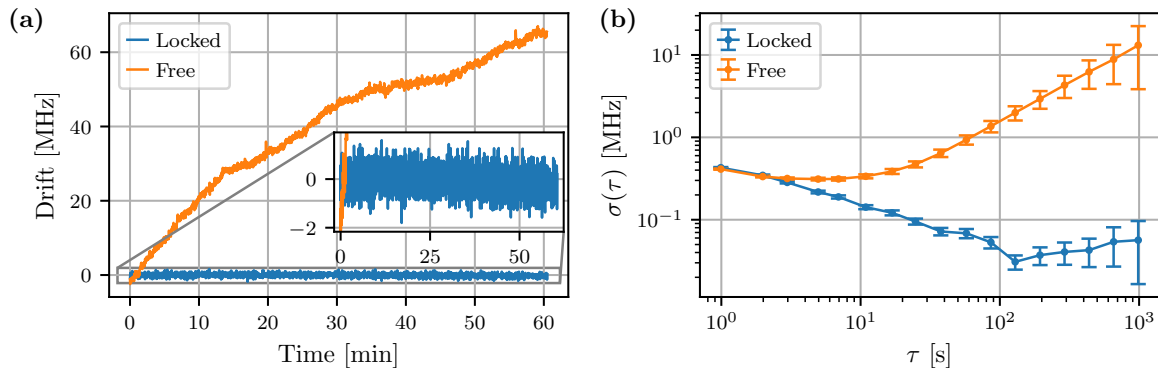


FIG. 4. Long-term frequency stability of a laser that is locked by the STCL. **(a)** Frequency drifts of a laser with (Locked) and without (Free) the STCL engaged over the course of an hour. This data has been evaluated from beat-note measurements relative to an additional frequency-stabilized reference laser. Significant frequency variations of the laser are suppressed by the locking system. **(b)** Allan deviation $\sigma(\tau)$ of the frequency stabilized laser in (a) for increasing averaging times τ .

of around 20 minutes. Frequency jumps on the order of 15 MHz indicate the times when the lock was manually engaged and disengaged. Residual high frequency noise visible on the signal was due to the inherent noise of the home-built laser. We find that the maximum time for which the lock can operate is mainly limited by the thermal drifts of the cavity, which can at some point exceed the tuning range of the piezo actuators. In a temperature stabilized labspace, we have observed this time to exceed several hours.

C. Stability against perturbations

We further investigated the effects of sudden perturbations on the performance of the STCL using a similar setup as in the previous section. For this, the locked laser was strongly perturbed by manually knocking the optical table or by adding current spikes to the diode laser current while the lock was engaged. The resulting monitoring signal is shown in Fig. 3b. Occasional jumps in the signal reach 70 MHz and correspond to the times when the laser was perturbed. Such jumps were well within the pre-defined region of interest for the peak detection of this laser. Therefore, the STCL could always detect the resonance, the resulting frequency spikes were quickly reduced again and the laser remained locked throughout the test, without any significant drift.

We note that any perturbations larger than the region of interest, such as laser mode-hops, can still interrupt the lock. This is particularly important to keep in mind when more lasers are added to the same cavity, which limits the size of the region of interest available for each laser.

D. Scalability

In order to test the scalability of our STCL scheme, we locked up to four lasers simultaneously on a single transfer cavity. Including the monitoring RP, a total of four RP units were used for the frequency stabilization of the lasers L1 to

L4. For demonstration purposes, the resonances of the lasers were spaced equally throughout the scanned range. The wavelengths corresponded again to the cooling scheme for barium monofluoride [28], which features transitions between 860 nm and 898 nm. The monitored error signals are summarized in Fig. 3c, with only the first 5 minutes shown for clarity. All four lasers were successfully stabilized against any relevant frequency drifts on timescales exceeding hours.

V. PERFORMANCE

To characterize the long-term performance of the STCL, we used a beat note of two overlapped lasers. An example is given in Fig. 4, where the two lasers were realized using commercial diode lasers. One of these lasers, frequency stabilized via DAVLL [4] to the D2-line of ^{85}Rb , served as a precise reference for residual drifts of the second laser. This second laser was locked using the STCL to a frequency roughly 60 MHz away, allowing for a measurement of the beat-note signal using an oscilloscope with 200 MHz bandwidth. For the reference laser used in the STCL scheme, a separate third laser at the same wavelength was used, stabilized with a DAVLL scheme on the ^{87}Rb D2 line. The use of two lasers with wavelengths close to each other reduced drifts caused by environmental factors for the STCL [20]. Moreover, the choice of a separate reference laser for the beat-note measurement assured that the measurements were not influenced by drifts of the reference laser.

The beat-note signal was acquired with a frequency of 1 Hz over the course of an hour. Variations in the frequency of the laser were evaluated by the peak positions of the Fourier-transformed signals. The resulting frequency drift Δf is shown in Fig. 4a. Without engaging the transfer lock, the frequency of the laser drifts by more than 60 MHz over the course of one hour. These drifts were fully compensated while the STCL was engaged. Notably, the frequency drifts over an hour were characterized by a standard deviation of 0.5 MHz, well below the short-term fluctuations of the indi-

vidual lasers. The largest residual drifts observed in a large set of such test measurements performed over several weeks of operation were on the order of 1.5 MHz. The Allan deviation calculated from the measured frequency drifts $\sigma(\tau)$ is shown in Fig. 4b. For increasing averaging times τ up to 200 s, $\sigma(\tau)$ decreases due to averaging of short-term noise. For longer τ , an upwards trend indicates the effect of the small residual frequency drifts.

Substituting the STCL's reference with a frequency stabilized helium-neon laser resulted in a similar performance with drifts of 0.8 MHz over three hours, which can be explained by both a temperature drift around 0.5°C during the measurement and the specified frequency stability of the helium-neon laser of 1 MHz per hour.

VI. CONCLUSION

We have used the capabilities of the *STEMlab* platform provided by *Red Pitaya* to develop a STCL that is both cost-efficient and scalable. To prevent an overhead in data-transfer, *Python* modules were developed to implement the signal processing and feedback loop digitally directly on the RP's CPU with a bandwidth of up to 100 Hz. The STCL is remotely accessible from a PC, allowing the control and monitoring of the individual laser locks. Its scalability has been demonstrated by simultaneous stabilization of four lasers on a single cavity. We determined the long-term stability of the system to stay well below 1 MHz over the course of an hour. These parameters make our STCL particularly useful for the laser cooling of many molecular species.

ACKNOWLEDGMENTS

We are indebted to Tilman Pfau for generous support and thank Max Mäusezahl for fruitful discussions and advice on the amplifiers used to drive the piezo actuators [27]. This project has received funding from the European Research Council (ERC) under the European Union's Horizon 2020 research and innovation programme (Grant agreements No. 949431), Vector Stiftung, the RiSC programme of the Ministry of Science, Research and Arts Baden-Württemberg and Carl Zeiss Foundation.

DATA AVAILABILITY STATEMENT

The *Python* codes used in this study are openly available in the GitHub repository of the Langen Group [29].

Appendix A: Removing overlapping cavity transmission peaks from different lasers

As shown in the main text, many lasers can be coupled into the same cavity to stabilize them using the STCL. In principle, this only requires sufficient power to reliably detect the

transmission peak of each laser. The robustness of the STCL, however, depends on the size of the region of interest available around each transmission peak to uniquely detect and compensate the frequency fluctuations of the corresponding laser. Therefore the spacing between the individual peaks in the cavity transmission signal effectively limits the maximum number of lockable lasers. In particular, overlapping resonances from different lasers can easily interfere with the successful operation of the frequency stabilization algorithm.

For this reason, the cavities used in our work are equipped with an additional piezo actuator to control the overall length of the cavity independent of the scanning piezo actuator that participates in the lock. When scanning the length L of the resonator using this latter piezo actuator, the free spectral range of different lasers depends on their wavelength according to the standing wave condition $L = m\lambda/2, m \in \mathbb{N}$. This wavelength dependence allows us to tune the relative resonance positions of different lasers by choosing an appropriate scan range with the second piezo. This is demonstrated in Fig. 5. Effectively, the mode number m is shifted by Δm for all lasers. The change in relative position to the reference peak for a laser L can then be modeled as $(\lambda_L/\lambda_{\text{Ref}} - 1)\Delta t_{\text{FSR}} \times \Delta m$.

As an alternative to this approach, additional transfer cavities can be set up or the frequencies of the lasers can be shifted (e.g. using acousto-optical modulation) before coupling them into the cavity used for the STCL.

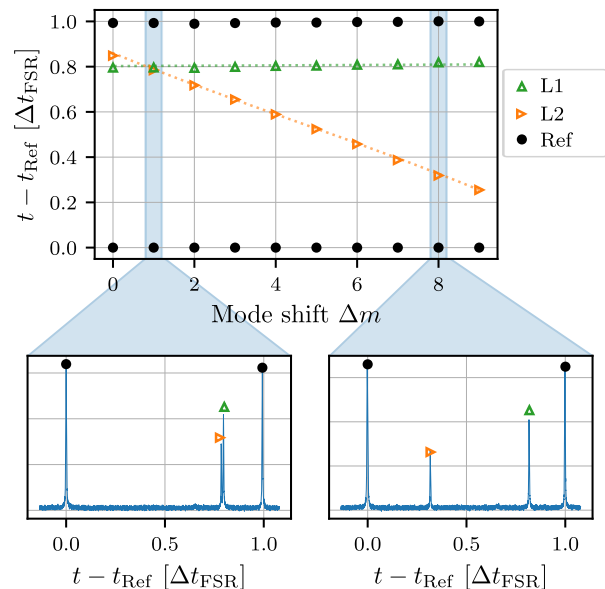


FIG. 5. Tunability of relative resonance positions. For the data shown, the piezo of an unstabilized cavity has been shifted over a range of 50 V. The visible peaks then correspond to resonances with mode numbers that are shifted by Δm . The relative peak positions for different mode shifts are determined from cavity signals as indicated in the insets. Dotted lines are a guide to the eye. Lasers L1 and L2 have wavelengths of 828 nm and 896 nm, respectively. By offsetting the cavity length, neighboring resonances (left inset, $\Delta m = 1$) of L1 and L2 can be well separated (right inset, $\Delta m = 8$).

-
- [1] C. Wieman and T. W. Hänsch, *Phys. Rev. Lett.* **36**, 1170 (1976).
- [2] G. C. Bjorklund, M. D. Levenson, W. Lenth, and C. Ortiz, *Applied Physics B* 1983 32:3 **32**, 145 (1983).
- [3] C. P. Pearman, C. S. Adams, S. G. Cox, P. F. Griffin, D. A. Smith, and I. G. Hughes, *Journal of Physics B: Atomic, Molecular and Optical Physics* **35**, 5141 (2002).
- [4] K. L. Corwin, Z.-T. Lu, C. F. Hand, R. J. Epstein, and C. E. Wieman, *Appl. Opt.* **37**, 3295 (1998).
- [5] T. Hansch and B. Couillaud, *Optics Communications* **35**, 441 (1980).
- [6] R. W. Drever, J. L. Hall, F. V. Kowalski, J. Hough, G. M. Ford, A. J. Munley, and H. Ward, *Applied Physics B* 1983 31:2 **31**, 97 (1983).
- [7] E. D. Black, *American Journal of Physics* **69**, 79 (2001).
- [8] J. Alnis, A. Matveev, N. Kolachevsky, T. Udem, and T. W. Hänsch, *Physical Review A* **77**, 053809 (2008).
- [9] W. Zhang, J. M. Robinson, L. Sonderhouse, E. Oelker, C. Benko, J. L. Hall, T. Legero, D. G. Matei, F. Riehle, U. Sterr, and J. Ye, *Phys. Rev. Lett.* **119**, 243601 (2017).
- [10] T. Bothwell, C. J. Kennedy, A. Aeppli, D. Kedar, J. M. Robinson, E. Oelker, A. Staron, and J. Ye, *Nature* **602**, 420 (2022).
- [11] P. Kwee, C. Bogan, K. Danzmann, M. Frede, H. Kim, P. King, J. Pöld, O. Puncken, R. L. Savage, F. Seifert, P. Wessels, L. Winkelmann, and B. Willke, *Opt. Express* **20**, 10617 (2012).
- [12] M. R. Tarbutt, *Contemporary Physics* **59**, 356 (2018), arXiv:1902.05628.
- [13] T. Langen, G. Valtolina, D. Wang, and J. Ye, "Quantum state manipulation and science of ultracold molecules," (2023), arXiv:2305.13445 [cond-mat.quant-gas].
- [14] F. Kogel, M. Rockenhäuser, R. Albrecht, and T. Langen, *New Journal of Physics* **23**, 095003 (2021), arXiv:2106.13177.
- [15] N. B. Vilas, C. Hallas, L. Anderegg, P. Robichaud, A. Winnicki, D. Mitra, and J. M. Doyle, *Nature* **606**, 70 (2022).
- [16] RedPitaya STEMLab 125-14, <https://redpitaya.com>.
- [17] B. E. A. Saleh and M. C. Teich, *Fundamentals of photonics; 2nd ed.*, Wiley series in pure and applied optics (Wiley, New York, NY, 2007).
- [18] J. H. T. Burke, O. Garcia, K. J. Hughes, B. Livedalen, and C. A. Sackett, *Review of Scientific Instruments* **76**, 116105 (2005), <https://doi.org/10.1063/1.2135278>.
- [19] N. Seymour-Smith, P. Blythe, M. Keller, and W. Lange, *Review of Scientific Instruments* **81**, 075109 (2010).
- [20] S. Subhankar, A. Restelli, Y. Wang, S. L. Rolston, and J. V. Porto, *Review of Scientific Instruments* **90**, 043115 (2019), arXiv:1810.07256.
- [21] D. Wang, W. Bu, D. Xie, T. Chen, and B. Yan, *J. Opt. Soc. Am. B* **35**, 1658 (2018).
- [22] A. Matsushima, *Transverse Laser Cooling of SrF*, Phd thesis, Imperial College (2013).
- [23] J. Barry, *Laser cooling and slowing of a diatomic molecule*, Phd thesis, Yale University (2013).
- [24] L. Neuhaus, R. Metzdorff, S. Chua, T. Jacqmin, T. Briant, A. Heidmann, P.-F. Cohadon, and S. Deleglise, in *2017 Conference on Lasers and Electro-Optics Europe & European Quantum Electronics Conference (CLEO/Europe-EQEC)*, Vol. Part F81-E (IEEE, 2017) pp. 1–1.
- [25] R. W. Schafer, *IEEE Signal Processing Magazine* **28**, 111 (2011).
- [26] C. Tomschitz, *A photoionization scheme to create cold ionic impurities from Rydberg atoms*, Master's thesis, University of Stuttgart (2018).
- [27] M. Mäusezahl, F. Munkes, and R. Löw, Submitted to *New Journal of Physics* as an invited review/tutorial for the special issue "Focus on Hot Atomic Vapors" (2023).
- [28] R. Albrecht, M. Scharwaechter, T. Sixt, L. Hofer, and T. Langen, *Physical Review A* **101**, 013413 (2020), arXiv:1906.08798.
- [29] E. Pultinevicius, M. Rockenhäuser, F. Kogel, P. Groß, T. Garg, O. E. Prochnow, and T. Langen, <https://github.com/LangenGroup/RedPitayaSTCL>.